

# Dependence of $\vec{p}\vec{p} \rightarrow pp\pi^0$ near Threshold on the Spin of the Colliding Nucleons

H.O. Meyer, J.T. Balewski, M. Dziedzic, J. Doskow, R.E. Pollock, B. v. Przewoski,  
T. Rinckel, F. Sperisen, P. Thörngren-Engblom, M. Wolanski  
*Dept. of Physics and Cyclotron Facility, Indiana University, Bloomington, Indiana 47405*

W. Haeberli, B. Lorentz, F. Rathmann\*, B. Schwartz, T. Wise  
*University of Wisconsin-Madison, Madison, WI, 53706*

W.W. Daehnick, R.W. Flammang, Swapan K. Saha†, D.J. Tedeschi‡  
*Dept. of Physics and Astronomy, University of Pittsburgh, Pittsburgh, PA 15260*

P.V. Pancella  
*Western Michigan University, Kalamazoo, MI, 49008*  
(August 27, 2019)

## Abstract

A polarized internal atomic hydrogen target and a stored, polarized beam are used to measure the spin-dependent total cross section  $\Delta\sigma_T/\sigma_{\text{tot}}$ , as well as the polar integrals of the spin correlation coefficient combination  $A_{xx} - A_{yy}$ , and the analyzing power  $A_y$  for  $\vec{p}\vec{p} \rightarrow pp\pi^0$  at four bombarding energies between 325 and 400 MeV. This experiment is made possible by the use of a cooled beam in a storage ring. The polarization observables are used to study the contribution from individual partial waves.

24.70.+s , 25.10.+s , 29.20.Dh , 20.25.Pj , 29.27.Hj

Typeset using REVTeX

---

\*present address: Forschungszentrum Jülich GmbH, 52425 Jülich, Germany.

†permanent address: Bose Institute, Calcutta 700009, India

‡Physics Department, Univ. of South Carolina, Columbia, SC 29208

Close to threshold, pion production in the nucleon-nucleon (NN) system involves only a few partial waves, because the relative kinetic energies between the particles in the final state are small. At the same time, the transferred momentum is large, making this reaction sensitive to the short-range NN interaction. This gives us the rare opportunity to study the NN interaction in a regime where the nucleons start to overlap, while being able to experimentally separate contributions from different angular momentum states. For instance, in  $pp \rightarrow pp\pi^0$ , the transition from a  ${}^3P_0$  initial state to a  ${}^1S_0$ ,  $l_\pi = 0$  final state (or short, Ss) can be isolated by lowering the bombarding energy until all higher partial waves have become insignificant. This is the case for bombarding energies below about 300 MeV. A measurement of the total cross section,  $\sigma_{\text{tot}}$ , in this regime [1,2] became possible with the advent of storage ring technology (for a review, see [3]). At the time of that measurement, calculations using the ansatz of Koltun [4] under-predicted the total cross section by about a factor of five. Subsequently it was suggested that off-shell rescattering [5], and an enhancement of the axial charge from the exchange of heavy mesons ( $\omega$ ,  $\sigma$ ) [6] are important processes which were previously omitted. First attempts were also made to relate this process to fundamental symmetries by use of chiral perturbation theory (Ref. [7], and references therein).

The present experiment uses a polarized beam on a polarized target to extend the study of the  $pp \rightarrow pp\pi^0$  reaction to the higher partial waves with p-wave nucleons and s-wave pions (short, Ps), or p-wave nucleons and pions (Pp) in the final channel (the combination Sp is forbidden). Bombarding energies were chosen to cover the range over which the higher partial waves gradually become significant, and finally dominate the reaction. Except for a few analyzing power data of low precision [8,9], this is the first investigation of polarization observables in this reaction below 400 MeV.

The experiment was carried out with the Indiana Cooler. Protons from the cyclotron were stack-injected into the ring at 197 MeV, reaching an orbiting current of several 100  $\mu\text{A}$  within a few minutes. The beam was then accelerated to the energies listed in Table 1. After typically 10 minutes of data taking, the remaining beam was discarded, and the cycle was repeated. The beam polarization was vertical, either up or down; the direction was inverted after each cycle.

Experience in the use of the polarized target and stored, polarized beam was gained during a series of precise measurements of spin correlation coefficients in pp elastic scattering [10]. The internal polarized target is realized by injecting a beam of polarized atoms into an open-ended storage cell (S in Fig. 1) which, for this experiment, consisted of a 12 mm diameter aluminum tube of 25  $\mu\text{m}$  wall thickness. Such a cell minimizes the amount of material close to the beam, and allows an unobstructed view of the full azimuthal range. The cell is coated with Teflon to avoid depolarization of atoms colliding with the wall. Its position can be adjusted remotely to minimize beam halo intercepting the cell wall. During data taking, the target polarization is changed every 2 s pointing in sequence, up, down, left, right. A target polarization change takes less than 100 ms and does not affect the magnitude of the polarization [10].

The detector arrangement is shown in Fig. 1. Reaction products from the target region exit the vacuum chamber through a 0.18 mm thick stainless steel foil (not shown). Two segmented scintillator arrays (E, K) with a total thickness of 25 cm are designed to stop the protons from  $pp \rightarrow pp\pi^0$  : if a particle reaches detector V, the event is vetoed. Outgoing

charged particles are identified by their energy and their time of flight between the F and E scintillators. Their direction is measured by a set of four wire planes (WC1, WC2). The detector setup is similar to the one used for the  $pp \rightarrow pp\pi^\circ$  total cross section measurement [1], with some changes to cover the larger angular range at the higher energies of this measurement. Typical distributions of the reconstructed mass,  $m_x$ , of the undetected particle are shown in Fig. 2. The events of interest are those in the  $\pi^\circ$  peak. The background under the peak (less than 10% of the total yield) is estimated using a background shape which is consistent with data obtained with only  $N_2$  gas in the target cell.

Proton-proton elastic scattering was used to monitor polarization and luminosity, concurrently with the acquisition of  $\bar{p}\bar{p} \rightarrow pp\pi^\circ$  events. To this end, coincidences between two protons exiting near  $\theta_{\text{lab}} = 45^\circ$  are detected by two pairs of scintillators placed at  $\Phi = \pm 45^\circ$  and  $\Phi = \pm 135^\circ$  (X in Fig. 1). For vertical beam and horizontal target polarization this arrangement measures the spin correlation coefficient combination  $A_{xx} - A_{yy}$  which, for pp scattering, is large and known [11]. This yields an accurate measurement of the product of beam and target polarization,  $P_{BT} \equiv P_B \cdot P_T$  (see Table 1). In addition, the time-integrated luminosity,  $\int L dt$ , is deduced from the known pp elastic cross section (see Table 1). After correcting for particles lost through the central hole (discussed below), the inefficiency of the wire chambers ( $\sim 7\%$ ), and the loss of events due to reactions in the scintillators (6-10%), we verified that the observed number of  $pp\pi^\circ$  events agrees with the total cross section in the literature, ranging from about  $8 \mu\text{b}$  at 325 MeV to  $70 \mu\text{b}$  at 400 MeV.

Data are acquired in all eight possible combinations of beam (up, down) and target polarization (up, down, left, right). As is clearly visible in Fig. 2, the total cross section depends on the polarization of the colliding protons, and the spin-dependent cross section,  $\Delta\sigma_T$  (defined as the cross section with the spins of the colliding protons vertical and opposite, minus the cross section with spins parallel) can be calculated in a straight-forward way from the corresponding four yields. The resulting values for  $\Delta\sigma_T/\sigma_{\text{tot}}$  are listed in Table 1, and shown in Fig. 3.

In this experiment, complete kinematic information is obtained for each event. Thus, spin-dependent observables other than  $\Delta\sigma_T$  can also be investigated. To demonstrate this, we sort the yields as a function of  $\varphi_\pi$ , the azimuthal angle of the  $\pi^\circ$ . The columns in Fig. 4 correspond to the four bombarding energies, and the rows to different combinations  $R_i$  of the spin-dependent yields (for instance,  $R_1 = (\text{sum of yields with beam spin up}) / (\text{sum of yields with beam spin down})$ ). The yields for different spin states are normalized to the same integrated luminosity. To obtain the plotted quantity, we calculate  $W_i = (R_i - 1) / (R_i + 1)$ , and divide by  $(P_{BT})^{1/2}$  for the first three rows, or  $P_{BT}$  for the last two rows. The last two rows reflect the spin correlation coefficient combinations  $S \equiv (A_{xx} + A_{yy})$ , and  $D \equiv (A_{xx} - A_{yy})$ , while the first three rows are related to the beam and target analyzing powers,  $A_y^B$  and  $A_y^T$ , namely  $a_B = A_y^B P_B / (P_{BT})^{1/2}$ , and  $a_T = A_y^T P_T / (P_{BT})^{1/2}$ . The latter are defined such that the product  $a_B \cdot a_T$  no longer depends on beam and target polarization. The solid lines in Fig. 4 represent a least square fit using the known  $\varphi_\pi$  dependence (listed to the right of Fig. 4), varying the four parameters  $a_B$ ,  $a_T$ ,  $S$ , and  $D$ . The fact that we ignore all kinematic variables, except  $\varphi_\pi$  means that we implicitly integrate over the variables of the two protons *and the pion polar angle*. The beam and target analyzing powers, integrated over  $\theta_\pi$ , are related by  $A_y^B = -A_y^T \equiv A_y$ . The integrated analyzing power is then obtained by calculating  $A_y = (-a_B \cdot a_T)^{1/2}$ . We note that the spin-dependent total cross section is

related to the integrated spin correlation coefficients by  $\Delta\sigma_T/\sigma_{tot} = -S$ . This quantity can be deduced more directly as described earlier, and the two analysis methods agree. The resulting polarization observables are listed in Table 1, and plotted in Fig. 3.

Our detector does not cover completely all of the phase space of the exit channel because of the central hole that accommodates the circulating beam, excluding particles with  $\theta_{lab} \leq 5^\circ$ , and causing a sizeable loss of events (about 30% at the lowest energy). This deficiency in acceptance was studied by artificially enlarging the hole, accepting only events with both protons outside a cone of opening angle  $\Theta_{hole}$ . The resulting dependence of  $\Delta\sigma_T/\sigma_{tot}$  on  $\Theta_{hole}$  is weak, and consistent with an estimate based on the difference in the geometrical acceptance for different exit channels. This difference is caused by the final state interaction in the Ss channel (see Ref. [1]) which enhances the part of phase space with protons of low relative kinetic energy, and which is absent in the Ps and Pp channels. This study yields a correction to  $\Delta\sigma_T/\sigma_{tot}$  of the size of about one standard deviation. Other possible systematic effects were found to be negligible. They include a difference between the up and the down polarization of the beam, a dependence of the acquisition dead time on the spin state, and reasonable variations of the selection criteria for valid events. The validity of the background subtraction is tested by varying the range of accepted masses  $m_x$ . A change of the subtracted background by  $\pm 25\%$  is used to estimate an error which is added in quadrature to the statistical errors, resulting in the errors listed in Table 1.

Polarization observables permit a detailed study of individual partial waves. In a first attempt to demonstrate this, we express the observables near threshold in terms of “partial wave” contributions,

$$\Delta\sigma_T/\sigma_{tot} = -2 + (U/\sigma_{tot})\eta^\alpha + (V_1/\sigma_{tot})\eta^\beta \quad (1)$$

$$A_{xx} - A_{yy} = (V_2/\sigma_{tot})\eta^\beta \quad (2)$$

$$A_y = (W/\sigma_{tot})\eta^{(\alpha+\beta)/2} \quad (3)$$

where U and  $V_{1,2}$  correspond to transitions to a Ps or a Pp final state, respectively, and W is due to interference between Ps and Pp. The unpolarized total cross section is from the literature. The energy dependence is described by a power law in  $\eta = p_{\pi,max}/m_\pi$ . The dotted lines in Fig. 3 are obtained with  $U = 98 \mu b$ ,  $V_1 = 105 \mu b$ ,  $V_2 = 32 \mu b$ ,  $W = -22 \mu b$ ,  $\alpha = 4.8$ , and  $\beta = 8$ . The energy dependence of the Pp transitions is well represented by  $\beta = 8$  (expected from phase space) but the Ps transitions show an energy dependence ( $\alpha$ ) that is weaker than the expected power of 6. Note, that at threshold ( $\eta = 0$ ),  $\Delta\sigma_T/\sigma_{tot}$  attains the theoretical limit of  $-2$ .

Most of the theoretical work on  $pp \rightarrow pp\pi^0$  deals with the lowest partial wave (Ss). In fact, we are aware of only one calculation for  $\Delta\sigma_T$  that includes higher partial waves [12], the result of which is shown as a dashed line in Fig. 3. This calculation includes the exchange of heavy mesons, and provides a good fit to the total cross section below  $\eta = 0.5$  where the Ss final state dominates.

Here, we have reported first results from a study of spin dependence in  $\bar{p}\bar{p} \rightarrow pp\pi^0$ . More information will be obtained from an analysis in terms of different kinematic variables of the three-body final state, including angular distributions. Moreover, a measurement that involves *longitudinal* beam and target polarization is currently in progress. If history repeats itself this new and detailed information on one of the basic processes in nuclear

physics will prove as stimulating to the theoretical community as the earlier total cross section measurement [1].

### ACKNOWLEDGMENTS

We would like to thank the accelerator operations group for their efforts. We are also grateful to Ch. Hanhart for making the numerical values for the calculation shown in Fig. 3 available. This work has been supported by the US National Science Foundation under Grants PHY96-02872, PHY95- 14566, PHY97-22556, and by the US Department of Energy under Grant DOE-FG02-88ER40438.

## REFERENCES

- [1] H.O. Meyer et al., Nucl. Phys. A**539**, 633 (1992)
- [2] A. Bondar et al., Phys. Lett. B**356**, 8 (1995)
- [3] H.O. Meyer, Annu. Rev. Nucl. Part. Sci. **47**, 235 (1997)
- [4] D.S. Koltun and A. Reitan, Phys. Rev. **141** (1966) 1413
- [5] E. Hernandez and E. Oset, Phys. Lett. B**350**, 158 (1995)
- [6] T.S.H. Lee and D.O. Riska, Phys. Rev. Lett. **70**, 2237 (1993)
- [7] T. Sato, T.S.H. Lee, F. Myhrer and K. Kubodera, Phys. Rev. C**56**, 1246 (1997)
- [8] S. Stanislaus et al., Phys. Rev. C**44**, 2287 (1991)
- [9] G. Rappenecker et al., Nucl. Phys. A**590**, 763 (1995)
- [10] W. Haeblerli et al., Phys. Rev. C**55**, 597 (1997)
- [11] B. von Przewoski et al., Phys. Rev. C, in print
- [12] J. Haidenbauer, Ch. Hanhart and J. Speth, Acta Phys. Polonica B**27**, 2893 (1996)

## TABLES

TABLE I. Product of beam and target polarization, integrated luminosity, and the three measured polarization observables as a function of bombarding energy  $T$ , or  $\eta$  (maximum pion center-of-mass momentum divided by the pion mass). The observables in the last two columns are for a detected  $\pi^0$ , i.e., integrated over the variables of the two protons and the pion polar angle.

$T$ (MeV)	$\eta$	$P_B \cdot P_T$	$\int L dt$ $(\mu b)^{-1}$	$\Delta\sigma_T/\sigma_{tot}$ , or $-(A_{xx} + A_{yy})$	$A_{xx} - A_{yy}$	$A_y$
325.6	0.560	$0.456 \pm 0.003$	2163	$-1.038 \pm 0.075$	$-0.010 \pm 0.069$	$-0.066 \pm 0.018$
350.5	0.707	$0.342 \pm 0.004$	901	$-0.450 \pm 0.086$	$0.154 \pm 0.070$	$-0.160 \pm 0.023$
375.0	0.832	$0.514 \pm 0.004$	3024	$-0.285 \pm 0.021$	$0.230 \pm 0.023$	$-0.169 \pm 0.006$
400.0	0.948	$0.526 \pm 0.006$	831	$-0.070 \pm 0.046$	$0.245 \pm 0.030$	$-0.224 \pm 0.008$

# FIGURES

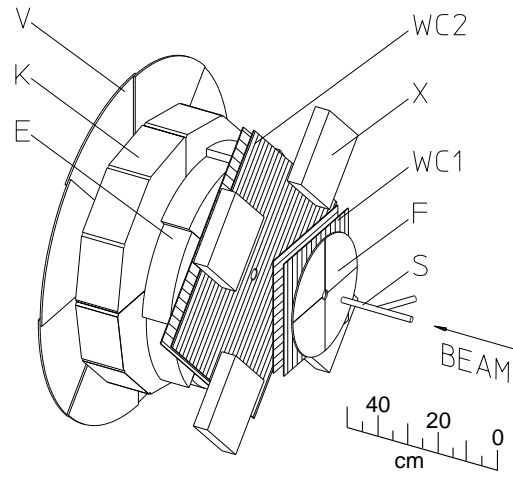


FIG. 1. Detector setup and storage cell target. The components are explained in the text.

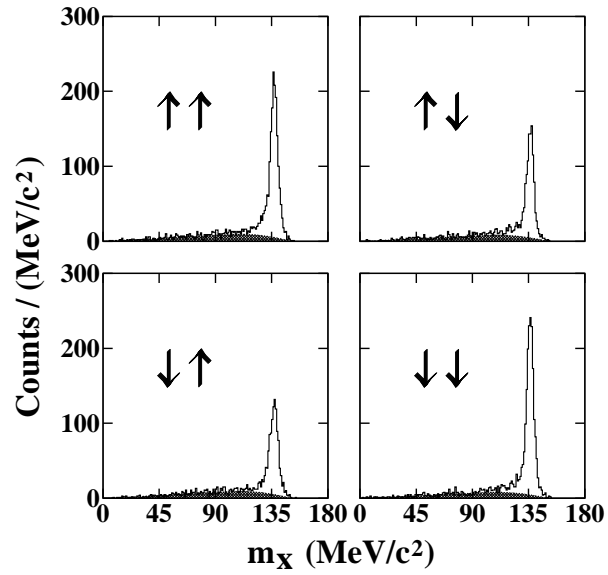


FIG. 2. Distributions of the calculated mass  $m_x$  of the undetected particle at 325 MeV bombarding energy, shown for the four combinations of vertical beam and target polarization. The peak of about  $7 \text{ MeV}/c^2$  FWHM occurs at the  $\pi^0$  rest mass. The shaded region indicates the assumed background distribution.

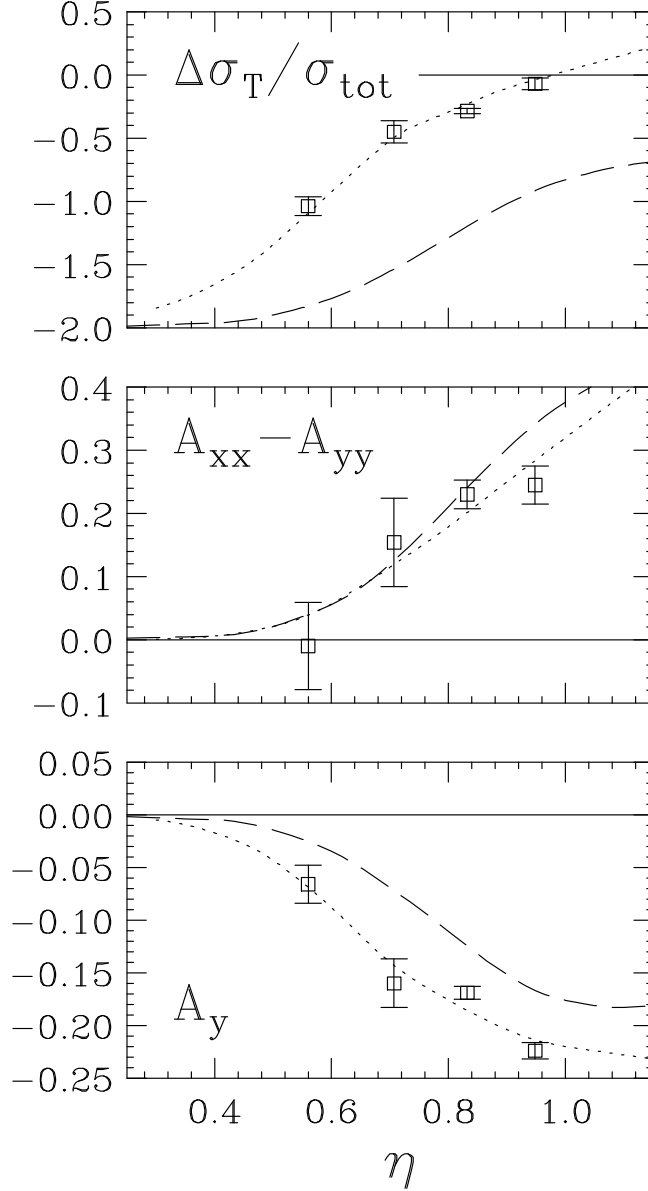


FIG. 3. The  $\bar{p}\bar{p} \rightarrow pp\pi^0$  polarization observables  $\Delta\sigma_T/\sigma_{\text{tot}} = -(A_{xx} + A_{yy})$ ,  $(A_{xx} - A_{yy})$  and  $A_y$  as listed in Table 1 versus  $\eta$ , the maximum pion center-of-mass momentum in units of the pion mass. The observables  $A_{xx}$ ,  $A_{yy}$  and  $A_y$  are integrated over the variables of the two protons and the pion polar angle. The dashed lines represent a meson-exchange calculation [12], and the dotted line is a partial-wave fit (explained in the text).

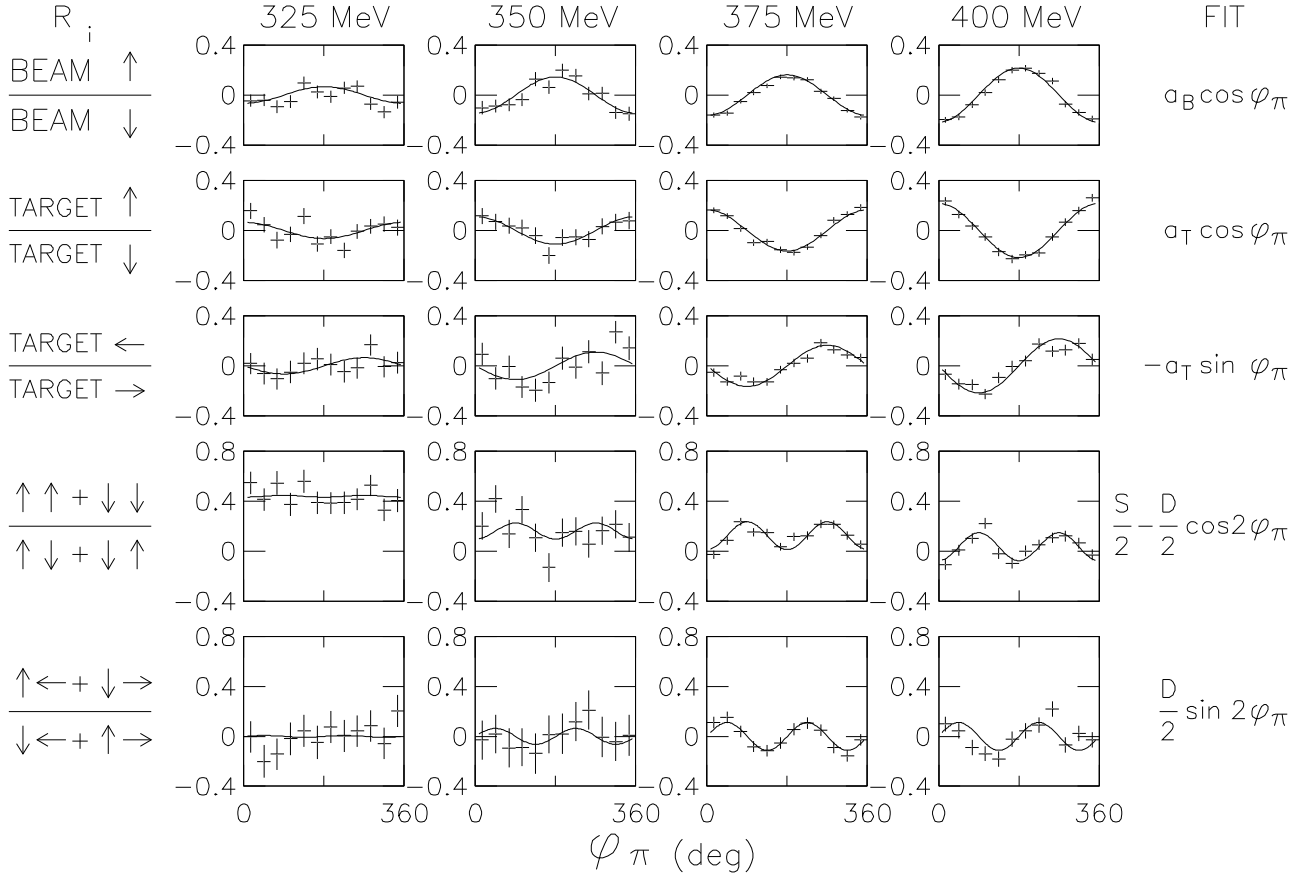


FIG. 4. Asymmetries for different spin combinations  $R_i$  (listed on the left) as a function of the azimuthal angle of the  $\pi^0$ . The solid curves are obtained from a least-square fit using the theoretical  $\varphi_\pi$  dependence (listed on the right), varying  $a_B$ ,  $a_T$ ,  $S \equiv (A_{xx} + A_{yy})$ , and  $D \equiv (A_{xx} - A_{yy})$ .